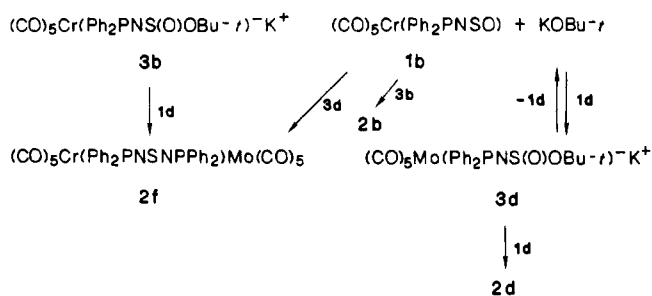
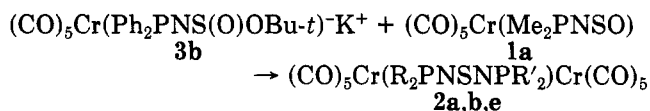


Scheme I



the temperature (Table V). This suggests that these two groups are in *cis* and *trans* conformations, respectively; i.e., only one isomeric form of **2e** exists at low temperature.



R = R' = Me, **2a**; R = R' = Ph, **2b**; R = Me, R' = Ph, **2e**

In order to explain the formation of all three products in these reactions we propose that dissociation of the potassium *tert*-butoxide adduct occurs as indicated in Scheme I for the formation of **2b**, **2d**, and **2f**. In support of this suggestion we observed the formation of **2b** when **3b** is heated alone at reflux in benzene.

Finally, when a solution of **3b** in benzene was heated at reflux in the presence of **2a**, a small quantity of **2e** (2%) was formed in addition to **2b**. We conclude from this result that a second mechanism, i.e. the reaction of sulfur diimide complexes with the potassium *tert*-butoxide adducts, plays a minor role in the determination of the final products in

the base-catalyzed condensation reactions of **1a-d**.

In summary, we have found that the reaction of $(\text{CO})_5\text{M}(\text{R}_2\text{PNSO})$ with potassium *tert*-butoxide is an excellent route to homodinuclear complexes of $\text{R}_2\text{PNSNPR}'_2$. Although this synthetic approach can be extended to the formation of heterodinuclear complexes of this ligand or homodinuclear complexes of the unsymmetrical ligand $\text{R}_2\text{PNSNPR}'_2$, the products are formed together with symmetrical products. The separation of these mixtures is difficult due to the similar solubility properties of all three products.

Acknowledgment. We thank the Natural Sciences and Engineering Research Council of Canada for financial support in the form of an operating grant (T.C.) and an infrastructure grant for the X-ray structural service. We are grateful to Professor M. Herberhold (Universität Bayreuth, W. Germany) for helpful correspondence and preprints of ref 3.

Registry No. **1a**, 108894-83-3; **1b**, 108894-84-4; **1c**, 108894-85-5; **1d**, 109007-84-3; **2a**, 108894-86-6; **2b**, 108894-87-7; **2c**, 108894-88-8; **2d**, 100815-29-0; **2e**, 108894-89-9; **2f**, 108894-90-2; **3a**, 108894-91-3; **3b**, 108894-92-4; **3d**, 108894-93-5; $(\text{CO})_5\text{Cr}(\text{Me}_2\text{PCL})$, 34629-15-7; $(\text{CO})_5\text{Cr}(\text{Ph}_2\text{PCL})$, 18461-36-4; $(\text{CO})_5\text{Mo}(\text{Me}_2\text{PCL})$, 34629-16-8; $(\text{CO})_5\text{Mo}(\text{Ph}_2\text{PCL})$, 23581-74-0; $(\text{CO})_5\text{Mo}(\text{Ph}_2\text{PNH}_2)$, 38268-63-2; $(\text{CO})_5\text{Cr}(\text{Me}_2\text{PNH}_2)$, 108894-94-6; $(\text{CO})_5\text{Cr}(\text{Ph}_2\text{PNH}_2)$, 108894-95-7; $(\text{CO})_5\text{Mo}(\text{Me}_2\text{PNH}_2)$, 38271-10-2; KNSO, 73400-02-9; K_2SN_2 , 82495-69-0; $\text{KOBu}-t$, 865-47-4; Me_2PCL , 811-62-1; Ph_2PCL , 1079-66-9; Me_2PNSO , 108836-37-9; Ph_2PNSO , 108836-38-0; $\text{Me}_2\text{PNHS}(\text{O})\text{OBu}-t$, 108836-39-1; $\text{Ph}_2\text{PNHS}(\text{O})\text{OBu}-t$, 108836-40-4.

Supplementary Material Available: Listings of positional and thermal parameters and all bond distances and bond angles (3 pages); a listing of observed and calculated structure factors (13 pages). Ordering information is given on any current masthead page.

Small-Ring Cyclic Cumulenes: Synthesis and X-ray Crystal Structure of Bis(triphenylphosphine)chloro(η^2 -1,2,3-cyclonatriene)rhodium

Richard O. Angus, Jr., Musiri N. Janakiraman, Robert A. Jacobson, and Richard P. Johnson*†

Department of Chemistry and Ames Laboratory—USDOE, Iowa State University, Ames, Iowa 50011

Received May 19, 1986

Reaction of the strained cumulene 1,2,3-cyclonatriene (**1**) with Wilkinson's catalyst (**2**; chlorotris(triphenylphosphine)rhodium) yields an air-stable crystalline complex (**6**). The complex shows a cumulenic infrared absorption at 1992 cm^{-1} . Complex **6** crystallizes in the orthorhombic space group *Pbca* (No. 61) with $a = 23.629$ (6) Å, $b = 23.912$ (30) Å, $c = 13.173$ (8) Å, and $Z = 8$. The X-ray crystal structure shows that the cumulene is complexed via the in-plane central double bond and is *trans* to the chlorine atom. C-7 of the cyclic cumulene shows two distinct locations in the crystal structure (50% probability each), which is best described in terms of a "flapping" disorder.

Introduction

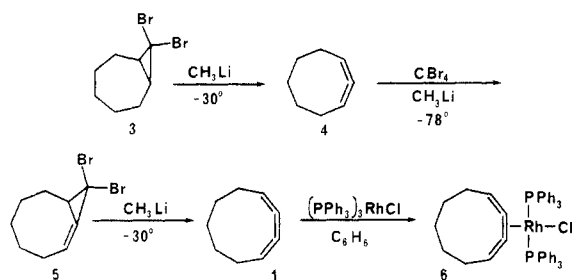
We have recently reported the synthesis and characterization of 1,2,3-cyclonatriene (**1**), which may be the smallest isolable cyclic butatriene.^{1,2} Molecular orbital

calculations led to the prediction that the normally linear butatriene moiety should be bent ca. $15-19^\circ$ in **1**, due to



*To whom correspondence should be addressed at the Department of Chemistry, University of New Hampshire, Durham, NH 03824.

(1) Angus, R. O., Jr.; Johnson, R. P. *J. Org. Chem.* 1984, 49, 2880.

Scheme I. Preparation of Bis(triphenylphosphine)chloro- $(\eta^2-1,2,3\text{-cyclononatriene})\text{rhodium}$

Table I. Crystal Data for $\text{RhCl}(\text{PPh}_3)_2\text{C}_9\text{H}_{12}$ (6)

mol formula	$\text{RhClP}_2\text{C}_{45}\text{H}_{42}$
fw	783.14
cryst system	orthorhombic
space group	<i>Pbca</i> (No. 61)
<i>a</i> , Å	23.629 (6)
<i>b</i> , Å	23.912 (30)
<i>c</i> , Å	13.173 (8)
<i>V</i> , Å ³	7442.77 (10.66)
<i>Z</i> (no. of molecules/unit cell)	8
$\mu(\text{Mo K}\alpha)$, cm ⁻¹ (correctn applied)	13.99
ρ_{calcd} g/cm ³	1.397
temp, °C	25
diffractometer	Syntex P2 ₁
monochromator	oriented graphite-incident beam
radiation	Mo K α ($\lambda = 0.71069$ Å)
reflectns measd	<i>hkl</i> , <i>hkl</i> (two octants)
scan type	ω -step scan
no. of std reflectns	1, measured every 100 reflectns
reflectns collected	13 912
reflectns obsd	3247 ($I > 3\sigma(I)$)
max 2θ , deg	50
min 2θ , deg	3.5
max no. of parameters refined	440
<i>R</i> (conventional)	0.048
<i>R_w</i> (weighted)	0.065
largest peak on final diff electron density map, e Å ⁻³	1.68
range of transmissn factors	0.96–0.95
agreement on averaged data	0.028

ring constraints. Although cold, dilute solutions of **1** are stable for at least several days, concentration, prolonged standing, or exposure of **1** to oxygen results in the formation of oligomeric material. In order to further characterize this novel cyclic butatriene, it seemed desirable to prepare a stable crystalline derivative. Butatrienes are known to form a variety of stable π complexes. Stang and co-workers have recently reported that Wilkinson's catalyst, chlorotris(triphenylphosphine)rhodium (**2**) forms stable η^2 complexes with linear butatrienes.⁴ We report here on the synthesis and X-ray crystal structure of the complex of **2** with 1,2,3-cyclononatriene (**1**).

Results and Discussion

1,2,3-Cyclononatriene (**1**) was prepared (Scheme I) as described in our previous report.¹ Reaction of a freshly prepared benzene solution of **1** with chlorotris(triphenylphosphine)rhodium (**2**) at ambient temperature gave (Scheme I) an air-stable crystalline solid (mp 148–151 °C) in 57% yield (based on **2**), after silica gel chromatog-

Table II. Atomic Coordinates ($\times 10^4$) and Average Temperature Factors ($\text{Å}^2, \times 10^3$) for $\text{RhCl}(\text{PPh}_3)_2\text{C}_9\text{H}_{12}$ (6)

atom	<i>x</i>	<i>y</i>	<i>z</i>	<i>U</i> (av)
Rh1	3235 (1)	1422 (1)	4180 (1)	35 (0)
Cl1	3268 (1)	413 (1)	4342 (2)	28 (0)
P1	2261 (1)	1368 (1)	4467 (2)	36 (0)
P2	4197 (1)	1398 (1)	3797 (2)	38 (0)
C1	2003 (4)	1093 (4)	5677 (7)	37 (3)
C2	2360 (4)	739 (4)	6237 (8)	47 (3)
C3	2169 (5)	546 (4)	7175 (8)	55 (4)
C4	1634 (4)	690 (4)	7546 (9)	56 (3)
C5	1293 (5)	1026 (5)	6984 (9)	66 (4)
C6	1476 (5)	1230 (5)	6028 (8)	56 (4)
C7	1843 (4)	2013 (4)	4352 (8)	45 (3)
C8	1872 (5)	2402 (4)	5142 (9)	61 (4)
C9	1563 (5)	2896 (5)	5062 (11)	74 (5)
C10	1217 (6)	2998 (5)	4197 (11)	91 (6)
C11	1187 (6)	2619 (5)	3445 (11)	88 (6)
C12	1494 (5)	2107 (5)	3494 (9)	63 (4)
C13	1950 (4)	905 (4)	3527 (7)	40 (3)
C14	1539 (5)	510 (5)	3734 (9)	59 (4)
C15	1306 (5)	181 (6)	2991 (9)	77 (5)
C16	1487 (5)	252 (5)	1987 (10)	71 (4)
C17	1900 (5)	629 (5)	1748 (9)	67 (4)
C18	2138 (5)	956 (4)	2520 (9)	59 (4)
C19	4608 (4)	1032 (4)	4753 (8)	40 (3)
C20	5159 (4)	811 (4)	4526 (9)	53 (3)
C21	5464 (5)	546 (4)	5296 (9)	61 (4)
C22	5243 (5)	504 (4)	6248 (10)	68 (4)
C23	4690 (5)	735 (4)	6492 (9)	63 (4)
C24	4382 (4)	992 (4)	5719 (8)	52 (3)
C25	4559 (4)	2070 (4)	3690 (9)	51 (4)
C26	4869 (5)	2284 (5)	4513 (9)	66 (4)
C27	5091 (6)	2821 (5)	4512 (11)	82 (5)
C28	5033 (5)	3138 (5)	3627 (12)	88 (6)
C29	4723 (5)	2920 (5)	2775 (11)	79 (5)
C30	4482 (5)	2381 (4)	2830 (9)	58 (4)
C31	4370 (4)	1058 (4)	2584 (8)	51 (3)
C32	4907 (5)	1167 (6)	2127 (9)	83 (5)
C33	5000 (7)	895 (6)	1152 (9)	101 (6)
C34	4590 (7)	552 (5)	727 (11)	98 (6)
C35	4073 (7)	455 (6)	1213 (10)	97 (6)
C36	3952 (6)	709 (4)	1237 (8)	64 (4)
C37	3246 (7)	3465 (6)	3116 (12)	103 (6)
C38	2814 (6)	3076 (5)	2653 (13)	99 (6)
C39	2925 (5)	2443 (5)	2807 (10)	70 (4)
C40	3128 (4)	2216 (4)	3641 (8)	47 (3)
C41	3312 (4)	2245 (4)	4614 (8)	49 (3)
C42	3501 (5)	2506 (5)	5427 (9)	66 (4)
C43	3575 (7)	3136 (5)	5505 (13)	107 (7)
C44	3147 (8)	3467 (6)	5024 (13)	117 (7)
C45	2811 (10)	3418 (10)	4262 (18)	63 (0) ^a
C45'	3627 (10)	3433 (10)	3947 (18)	63 (0) ^a

^a Assigned and not refined. The multipliers for C45 and C45' are 0.47 (2) and 0.53 (2), respectively.

raphy. Spectral data were consistent with those for structure **6**. The infrared spectrum of the complex displayed an absorption at 1992 cm⁻¹, which is attributable to the cumulenenic moiety. A similar band is not observed in uncomplexed **1**, probably because of its high symmetry. The 300-MHz ¹H NMR spectrum of **6** showed two narrow triphenylphosphine resonances (δ 7.7 and 7.3; ratio 1:2), a narrow multiplet (δ 5.3) for the vinyl hydrogens, and three symmetrical multiplets (δ 1.5, 0.6, and -0.06; ratio 4:4:2) for methylene groups. The C-7 methylene resonance in **6** is shifted 1.62 ppm upfield relative to **1**, presumably due to shielding by proximate phenyl groups in the triphenylphosphine ligand. Low-temperature (to 190 K) NMR experiments did not improve resolution. The UV spectrum showed maxima at 266 and 365 nm. The fast atom bombardment (FAB) mass spectrum for **6** was obtained in a matrix of *o*-nitrophenyl octyl ether. Although no parent ion was detectable, peaks were observed at *m/e* 747 (*M* - Cl), 662 (*M* - C₉H₁₂), and 627 (*M* - Cl - C₉H₁₂).

(2) For a review of structural limitations in cyclic cumulenes, see: Johnson, R. P. In *Molecular Structure and Energetics*; Greenberg, A., Liebman, J., Eds.; VCH Publishers: Deerfield Beach, FL, 1986; Vol. 3, p 85.

(3) Johnson, C. K. ORTEP, Report ORNL-3794, 1965; Oak Ridge National Laboratory, Oak Ridge, TN.

(4) Stang, P. J.; White, M. R.; Maas, G. *Organometallics* 1983, 2, 720.

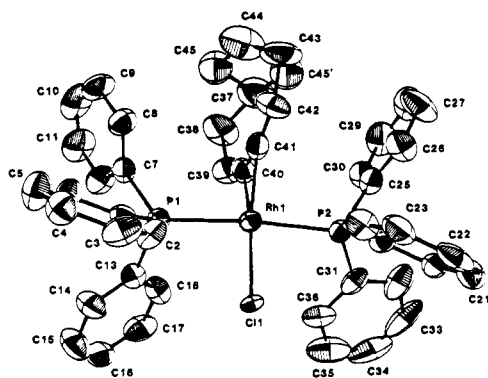


Figure 1. ORTEP structure for complex 6. Hydrogen atoms are omitted for clarity.

Table III. Selected Bond Distances (Å) and Bond Angles (deg)

Bond Distances			
Rh1-Cl1	2.421 (2)	C40-C41	1.356 (14)
Rh1-P1	2.335 (3)	C41-C42	1.316 (16)
Rh1-P2	2.330 (3)	C42-C43	1.521 (19)
Rh1-C40	2.046 (10)	C43-C44	1.431 (22)
Rh1-C41	2.062 (10)	C44-C45	1.285 (28)
C37-C38	1.509 (21)	C44-C45'	1.819 (28)
C38-C39	1.551 (19)	C45-C37	1.830 (28)
C39-C40	1.316 (14)	C45'-C37	1.420 (28)
Bond Angles			
Cl1-Rh1-P1	88.0 (1)	C37-C38-C39	115.7 (12)
Cl1-Rh1-P2	88.0 (1)	C38-C39-C40	125.1 (11)
Cl1-Rh1-C40	163.7 (3)	C39-C40-C41	152.2 (11)
Cl1-Rh1-C41	157.7 (3)	C40-C41-C42	154.5 (11)
P1-Rh1-P2	174.5 (1)	C41-C42-C43	124.3 (11)
P1-Rh1-C40	89.1 (3)	C42-C43-C44	115.8 (13)
P1-Rh1-C41	95.4 (3)	C43-C44-C45	137.1 (18)
P2-Rh1-C40	93.8 (3)	C43-C44-C45'	83.1 (12)
P2-Rh1-C41	89.7 (3)	C44-C45-C37	107.0 (17)
Rh1-C40-C39	137.1 (9)	C44-C45'-C37	101.7 (15)
Rh1-C40-C41	71.3 (6)	C45-C44-C45'	76.8 (15)
Rh1-C41-C40	70.1 (6)	C45-C37-C45'	73.6 (14)
Rh1-C41-C42	136.8 (9)	C38-C37-C45'	135.1 (15)
		C45-C37-C38	85.2 (12)

The structure of rhodium complex 6 was unambiguously determined by single-crystal X-ray diffraction. An ORTEP drawing³ of the complex is given in Figure 1. Tables I-III list crystal data, final fractional coordinates and average temperature factors for non-hydrogen atoms, and selected bond lengths and bond angles, respectively.

The crystal structure clearly reveals the η^2 -olefin bonding, as observed in other rhodium-butatriene complexes.⁴ Coordination about the rhodium is best described as square-planar, with the least-squares plane of the cumulene moiety skewed ca. 8° from perpendicularity to the P_2RhCl plane. Coordination of Rh to the central π bond is symmetrical (bond lengths of 2.046 (10) and 2.062 (10) Å) within experimental error.

In the complex, the butatriene ligand is held in a nearly C_2 conformation if the disordered C45 atom is omitted. Our previous MNDO calculations had predicted a slightly more stable C_s conformation for the uncomplexed 1. As expected, the central π bond in 6 is lengthened (C40-C41 = 1.356 Å) relative to 1 (1.269 Å predicted) and the butatriene remains strongly bent (150.9 and 152.6°). This ca. 30° cis bending is similar to that previously observed and greater than the bending predicted (162-165°) for conformations of 1.

One novel feature of the crystal structure is the disorder exhibited by the methylene carbon, C7 in butatriene 1. The difference electron density map revealed two positions, which are labeled as C45 and C45'. When these two

positions were input to the least-squares refinement, each with an occupancy factor of 0.5, little change from these values was noted (0.47 (2) and 0.53 (2), respectively, for C45 and C45'); this suggests nearly equal probability for the two locations. This also is reflected in the increasing of the size of the thermal ellipsoids as one moves around the ring from the rhodium side and in the relative constancy in the direction of the maximum amplitude of motion. This "flapping disorder" may be accounted for either by ambient temperature conformational mobility within the crystal or—perhaps more likely—the existence of two equally probable conformations.

In conclusion, 1,2,3-cyclononatriene (1) readily forms a crystalline complex by ligand displacement from Wilkinson's catalyst. The same should be true for other less stable cyclic butatrienes, and it may be possible to isolate these highly reactive molecules as rhodium complexes.⁵

Experimental Section

Bis(triphenylphosphine)chloro(2,3- η^2 -1,2,3-cyclononatriene)rhodium (6). 1,2,3-Cyclononatriene (1; 0.610 mmol) was prepared as described previously.¹ An ethereal solution of the butatriene (0.610 mmol; estimated by hydrogenation of an aliquot) was diluted with benzene (10 mL), concentrated to 5 mL under vacuum, and then diluted to 10 mL. A solution of tris(triphenylphosphine)chlororhodium (2; 283 mg, 0.305 mmol) in benzene (20 mL) was added, and the deep red solution was stirred under argon for 5 h. Concentration in vacuo, followed by chromatography over silica gel (elution with $CHCl_3/CCl_4$, 35:65), afforded 137 mg (57%) of yellow crystals: mp 148-151 °C; 300-MHz 1H NMR ($CDCl_3$) δ 7.70 (m, 10 H), 7.30 (m, 20 H), 5.30 (m, 2 H), 1.57 (m, 4 H), 0.63 (broadened pentet, $J \approx 6$ Hz, 4 H), -0.064 (broadened pentet, $J \approx 7$ Hz, 2 H); IR (CCl_4) 3088, 3072, 2935, 2864, 1992 (br), 1492, 1444, 1097, 751 cm^{-1} ; UV (THF) λ_{max} 226 nm (ϵ 3.7×10^4), 365 nm (ϵ 2.2×10^3); fast atom bombardment MS (ONPOE matrix) m/e 747 (M - Cl), 662 (M - C_9H_{12}), 627 (M - C_9H_{12} - Cl).

Crystallographic Summary for 6. Single crystals of 6 were grown from a solution of 6 in pentanes containing isoamyl acetate. A single pale yellow crystal of 6 with approximate dimensions of $0.05 \times 0.2 \times 0.4$ mm was mounted on a glass fiber and subsequently placed on a goniometer head. Twelve reflections ($9.5^\circ < 2\theta < 20^\circ$) were centered on a Syntex P2₁ automated diffractometer and indexed by the indexing program BLIND.⁶ A total of 13912 reflections (two octants of data) were collected by using an ω -step scan technique within a 2θ sphere of 50° and corrected for both Lorentz-polarization and absorption effects (an empirical absorption correction was made by using the method described by Karcher);⁷ 3247 independent reflections with $I \geq 3\sigma(I)$ were retained for use in subsequent calculations. The estimated variance in each intensity was calculated by $\sigma(I)^2 = C_T + C_B + (0.03C_T)^2 + (0.03C_B)^2 + (0.03I)^2$, where C_T and C_B represent the total and background counts, respectively, and the factor of 0.03 is an estimate of nonstatistical errors.

The position of the rhodium, chlorine, and the two phosphorus atoms were obtained from an ALCAMPS analysis⁸ of a superposition map, having selected a $(2x, 1/2, 1/2 - 2z)$ vector for a single superposition. All the remaining non-hydrogen atoms were found from successive structure factor and electron density map calculations. The difference map revealed "flapping disorder" for a carbon of the ligand (see Discussion). The positional and anisotropic thermal parameters for the non-hydrogen atoms were refined by a combination of block-matrix/full-matrix least-squares calculations.⁹ The positional parameters of the hydrogen atoms

(5) (a) Zoch, H.-G.; Sziemias, G.; Romer, R.; Schmitt, R. *Angew. Chem., Int. Ed. Engl.* 1981, 20, 877. (b) Schluter, A. D.; Belzner, J.; Heywang, V.; Sziemias, G. *Tetrahedron Lett.* 1980, 24, 891.

(6) Jacobson, R. A. *J. Appl. Crystallogr.* 1976, 9, 115.

(7) Karcher, B. A. Ph.D. Dissertation, Iowa State University, 1981.

(8) Richardson, J. W., Jr. Ph.D. Dissertation, Iowa State University, 1984.

(9) Lapp, R. L.; Jacobson, R. A. "ALLS, A Generalized Crystallographic Least-Squares Program", USDOE Report, 1979; Iowa State University, Ames, IA.

were calculated, were not varied during the refinement, and were all given a fixed isotropic temperature factor of 5.0 \AA^2 . The methylene hydrogen atoms on C37, C43, C44, C38, and C45 (C45') were not included in the refinement. The final conventional residual index ($R = \sum ||F_o| - |F_c|| / \sum |F_o|$) was 0.048 with a corresponding weighted index ($R_w = [\sum w(|F_o| - |F_c|)^2 / \sum w|F_o|^2]^{1/2}$) of 0.065, and the function minimized in the least-squares refinement was $\sum w(|F_o| - |F_c|)^2$, where $w = 1/\sigma(F)^2$. The atomic scattering factors were those from Ref. 10.

(10) (a) Cromer, D. T.; Weber, J. T. *International Tables for X-ray Crystallography*; Kynoch: Birmingham, England, 1974; Vol. IV, Table 2.2A, pp 71-79. (b) Templeton, D. H. *International Tables for X-ray Crystallography*; Kynoch: Birmingham, England, 1961; Vol. III, Table 3.3.2.c, pp 215-216.

Acknowledgment. X-ray diffraction studies were supported by the U.S. Department of Energy, Office of Basic Energy Sciences, Materials Sciences Division, under Contract No. W-7405-Eng-82. Synthetic studies received support from the donors of the Petroleum Research Fund, administered by the American Chemical Society.

Registry No. 1, 90885-93-1; 2, 14694-95-2; 6, 109086-50-2.

Supplementary Material Available: Tables of least-squares planes, bond lengths, bond angles, fractional coordinates of hydrogen atoms, and anisotropic thermal parameters of non-hydrogen atoms (5 pages); a list of calculated and observed structure factors (15 pages). Ordering information is given on any current masthead page.

Electronic Ground States and Isotropic Proton NMR Shifts of Manganocene and Its Derivatives

Daniel Cozak* and Francois Gauvin†

Department of Chemistry, Sciences and Engineering Faculty, Laval University, Quebec, Quebec, Canada G1K 7P4

Received January 16, 1987

A crossover enthalpy of $\Delta H^\circ = 21 \pm 5 \text{ kJ/mol}$ ($\Delta S^\circ = 100 \pm 20 \text{ J/(mol K)}$) for the slow spin exchange involving the ${}^6A_{1g} {}^2E_{2g}$ ground state of manganocene was found by paramagnetic NMR spectroscopy. A theoretical expression was derived which accounts for the average isotropic NMR shift in rapid exchanging molecules. In the case of dimethylmanganocene a fit with the experimental data was found for $\Delta H^\circ = 20 \text{ kJ/mol}$ ($\Delta S^\circ = 20 \text{ J/(mol K)}$) assuming an hyperfine spin coupling of 16 MHz for the thermally populated upper state of the complex. Both the molecular spin crossover enthalpies and the ring proton coupling constants found by NMR are consistent with a molecular ${}^2A_{1g}$ state dominated isotropic shift for dimethyl-, diethyl-, and tetraethylmanganocene. Hence, the large isotropic shift observed for the annular protons in the substituted complexes is explained by the rapid molecular exchange with the ${}^2A_{1g}$ state. Results show that for manganocene the slow exchange permits the observation of separate resonances as expected for the more populated ${}^2E_{2g}$ and ${}^6A_{1g}$ states. No resonance or evidence of an exchange with the ${}^2A_{1g}$ state was found between -90 and $110 \text{ }^\circ\text{C}$ for this complex.

Introduction

Generally, in paramagnetic transition-metal complexes the isotropic nuclear magnetic shifts of the ligand depends on the metal-ligand bonding and magnetic anisotropy. For metallocenes, spin density on the cyclopentadienyl rings will cause the carbon and its attached protons to experience a strong paramagnetic shift under nuclear magnetic resonance (NMR) experimental conditions. Most often the isotropic NMR shift is due either to spin density at the atom itself (contact interaction) or anisotropy originating from the neighboring metal center (dipolar interaction).

The molecular structure of several paramagnetic coordination compounds and organometallic metallocenes have been studied by proton and carbon NMR spectroscopy.¹ For the metallocenes of the transition series, the hyperfine coupling resulting from contact spin interaction can easily be obtained from the isotropic shift. Paramagnetic NMR has also been shown to be useful for the study of molecular dynamics. A good example of this is the diamagnetic/paramagnetic equilibrium for the $\text{Ni}(\text{PPh}_2\text{Me})_2\text{Br}_2$ complex.² Variable-temperature NMR studies have shown

that Ni(II) complexes have exchange-averaged isotropic shifts proportional to the mole fraction of thermally populated electronic state.^{3,4} Moreover, it has been shown that there is generally good agreement between the experimental and the theoretically predicted NMR bandwidths or isotropic shifts for fast exchanging ligands. This type of theoretical treatment of the isotropic NMR shifts is valid when each state follows the Curie law and is graphically significant for segments where the exchange-averaged shift is important relative to that of each state.⁴

These are $3d^5 \text{ Mn(II)}$ compounds with low enough crossover energies to allow for significantly populated doublet and sextet electronic ground states at experimentally accessible temperatures.⁵⁻⁹ Their NMR spectra

(1) *Applications of NMR in Paramagnetic Molecules*; La Mar, G. N., Horrocks, W. DeW., Jr., Holms, R. H., Eds.; Academic: New York, 1973; pp 1-678.

(2) Holms, R. H.; Hawkins, C. J. *Applications of NMR in Paramagnetic Molecules*; La Mar, G. N., Horrocks, W. DeW., Jr., Holms, R. H., Eds.; Academic: New York, 1973; p 243.

(3) Horrocks, W. DeW., Jr. *J. Am. Chem. Soc.* **1965**, *87*, 3779.

(4) Swift, T. J. *Applications of NMR of Paramagnetic Molecules*; La Mar, G. N., Horrocks, W. DeW., Jr., Holms, R. H., Eds.; Academic: New York, 1973; p 53.

(5) Hammett, J. H.; Bucher, R.; Oswald, N. *J. Am. Chem. Soc.* **1974**, *96*, 7833.

*Present address: Department of Chemistry, McGill University, 801 Sherbrooke Street W., Montreal, Quebec, Canada H3A 2K6.